Syntheses, Structures and Nonlinear Optical Properties of Ferrocenyl Complexes with Arylethenyl Substituents

José A. Mata,[a] Eduardo Peris,*[a] Rosa Llusar,[b] Santiago Uriel,[b] Marie P. Cifuentes,[c] Mark G. Humphrey,*[c] Marek Samoc,[d] and Barry Luther-Davies[d]

Keywords: Ferrocene / NLO / Bimetallic compounds / Crystal structure

The complexes (*E*)- and (*Z*)-Fe(η^5-C_5H_4CHO)(η^5-C_5H_4CH=CH–C_6H_4-4-NO_2) [**2**-(*E*) and **2**-(*Z*), respectively], (*E*)- and (*Z*)-Fe(η^5-C_5H_4CHO)(η^5-C_5H_4CH=CH–C_6H_4-4-CN) [**3**-(*E*) and **3**-(*Z*), respectively], (*E*,*E*)-, (*E*,*Z*)-, and (*Z*,*Z*)-Fe(η^5-C_5H_4CH=CHC_6H_4-4-NO_2)$_2$ [**4**-(*E*,*E*), **4**-(*E*,*Z*), and **4**-(*Z*,*Z*), respectively], (*E*,*E*)-, (*E*,*Z*)-, and (*Z*,*Z*)-Fe(η^5-C_5H_4CH=CHC_6H_4-4-CN)$_2$ [**5**-(*E*,*E*), **5**-(*E*,*Z*), and **5**-(*Z*,*Z*), respectively], and Fe(η^5-C_5H_5)(η^5-C_5H_4–(*E*)-CH=CH–4-{(η^6-C_6H_4)$Cr(CO)_3$}–(*E*)-CH=CH–η^5-C_5H_4)Fe(η^5-C_5H_5) (**7**) have been synthesized. Structural studies on **2**-(*E*), **4**-(*E*,*Z*), **5**-(*E*,*E*), Fe(η^5-C_5H_5){η^5-C_5H_4–(*E*)-CH=CH–4-C_6H_4–(*E*)-CH=CH–η^5-C_5H_4}Fe(η^5-C_5H_5) (**6**) and **7** have been performed. Electrochemical studies of **2**–**5** reveal trends in the oxidation potentials which are consistent with the more effective conjugation of the (*E*) isomers, and the better electron-accepting character of NO_2 than CN and of CHO than H. Powder SHG measurements by the Kurtz technique using fs pulses at the telecommunications wavelength of 1.3 μm reveal low responses for **4**-(*E*,*E*), **5**-(*E*,*E*), and **7**. Third-order NLO measurements by Z-scan using fs pulses at 800 nm suggest an increase in |γ| on increasing the electron-acceptor strength [when proceeding from **5**-(*E*,*Z*) to **4**-(*E*,*Z*), CN is replaced by NO_2], and on introduction of the $Cr(CO)_3$ unit, when proceeding from **6** to **7**.

Introduction

Ferrocene is a versatile building block. Its excellent thermal and photochemical stability, and combination of useful redox properties and chemical versatility, provides access to materials with potentially useful physical and chemical properties.[1–3] With the importance of ferrocene in the field of material science, there is currently great interest in the chemistry of ferrocenyl-based oligomers and ferrocenyl-containing conjugated compounds. The former contain the ferrocene building block in the repeat unit, and the latter couple ferrocene to a potentially π-delocalizable system. These complexes are of interest because of, amongst other things, their nonlinear optical (NLO) properties; the significant electron-donating strength of the ferrocenyl group has made it a good candidate for the design of chromophores with high NLO responses.

We previously reported on the syntheses, characterization, and molecular quadratic NLO behavior of ferrocene-containing conjugated compounds with pyridine, nitro, and nitrile pendant groups. This allowed us to obtain heterobimetallic complexes containing a series of electron-accepting moieties derived from $M(CO)_6$ (M = Cr, Mo, W) [Scheme 1 (a) and (b)].[4–6] Electrochemical studies together with the planar conformation of the molecular structures suggested effective electron delocalization along the conjugated chains. In a continuation of these studies, we have now synthesized a series of ferrocenyl 1,1′-bis-substituted complexes with nitro and nitrile pendant groups, whose electronic and solid-state structural properties have been studied. The results from these studies are reported herein. Similar 1,1′-bis-substituted ferrocenyl complexes with pendant pyridine groups have been reported by Lee et al., and show very interesting structural features.[7]

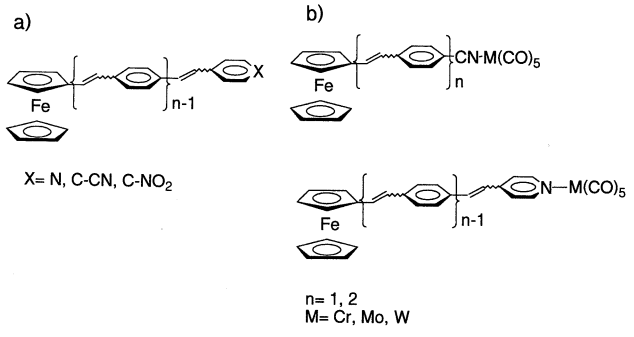

Scheme 1

We have also investigated arylethenyl-linked biferrocenes, with and without the presence of bridge arene-ligated $Cr(CO)_3$ units, the syntheses of which were reported by Müller et al.[8] while the current studies were underway. We

[a] Departamento de Química Inorgánica y Orgánica, Universitat Jaume I
Ctra. Borriol S/N, 12080 Castellón, Spain,
Fax: (internat.) +34 964/72 8214
E-mail: eperis@qio.uji.es
[b] Departamento de cc. Experimentales, Universitat Jaume I
Castellón, Spain
[c] Department of Chemistry, Australian National University
Canberra, ACT 0200, Australia
Fax: (internat.) +61 2/6125 0760
E-mail: Mark.Humphrey@anu.edu.au
[d] Australian Photonics Cooperative Research Centre, Laser Physics Centre, Research School of Physical Sciences and Engineering, Australian National University
Canberra, ACT 0200, Australia

  1434–1948/01/0808–2113 $ 17.50+.50/0

report herein a modified synthesis of the $Cr(CO)_3$-ligated complex, together with X-ray structural studies of both complexes.

Although the number of studies reporting second-order NLO responses of ferrocenyl complexes is very high, comparatively fewer studies exist in which third-order NLO responses are reported.[9] Since the effective delocalization in the molecular structures of our complexes fulfill a basic requirement for third-order NLO-active materials, we have measured and report herein on their cubic hyperpolarizabilities at 800 nm by Z-scan. While the bulk second-order susceptibilities of many ferrocenyl complexes have been reported,[10] much extant data has been obtained at wavelengths close to those of material resonances, resulting in significant resonance enhancement of the response. We therefore also report the bulk susceptibilities for these complexes by the Kurtz powder method at wavelengths remote from electronic absorption bands, thus enabling an assessment of off-resonance nonlinearity to be obtained.

Results and Discussion

Syntheses of 2−5

Based on our previous experience[4−6] we have synthesized compounds **2**−**5** by conventional Wittig and Horner−Emmons−Wadsworth methods (Scheme 2). The first step of the two-step reaction procedure afforded the bis-substituted complexes **2** and **3** with (*Z*) and (*E*) stereochemistry, together with small amounts of the bis-olefinated complexes (**4** and **5** in all their isomeric forms). Compounds **2** and **3** may be of interest in the design of new materials, since the presence of the carboxaldehyde group may provide access to a variety of functional groups. Complexes **2** and **3** undergo further olefination in the second step to yield **4** and **5** in all their isomeric forms [**4** and **5** exist as three isomers by combination of the (*E*) and (*Z*) dispositions of the vinylic group, i.e. (*E,E*), (*E,Z*) and (*Z,Z*)]. All three isomers were fully characterized for both the nitro and nitrile derivatives. Higher yields of the bis-substituted compounds **4** and **5** were obtained when performing the one-step (direct reaction) procedure. In all cases, separation of the (*E*) and (*Z*) isomers was easily achieved by column chromatography. Reaction of any of the complexes in refluxing toluene in the presence of iodine leads to the all-*E*-isomers in almost quantitative yields (see Experimental section).

Synthesis of 7

The synthesis of **6** was again based on Horner−Emmons−Wadsworth (HEW) olefinations using the corresponding phosphonate reagent. A synthesis of **7** was reported while the present studies were underway,[8] and involved olefination by HEW reaction of an η^6-coordinated carbonylchromium phenylene-bisphosphonate with ferrocenecarboxaldehyde. In the present study, η^6-coordination of the tri(carbonyl)chromium moiety to the phenylene bridging group of **6** was performed by heating compound **6** with $Cr(CO)_6$ in refluxing butyl ether (Scheme 3).

X-ray Structural Studies of 2-(*E*), 4-(*E,Z*), 5-(*E,E*), 6, and 7

The identities of **2**-(*E*) (ORTEP plots in Figures 1 and 2), **4**-(*E,Z*) (Figure 3), **5**-(*E,E*) (Figures 4 and 5), **6** (Figure 6), and **7** (Figure 7) were confirmed by single-crystal X-ray studies; crystallographic data are summarized in Table 5, and selected bond angles and distances are listed in Tables 1 and 2.

The structural studies reveal a number of interesting features. Complexes **2**-(*E*), **4**-(*E,Z*), and **5**-(*E,E*) provide the opportunity to assess the impact of π-system chain lengthening, stereochemistry, and acceptor modification on metrical parameters and crystal packing preference. In

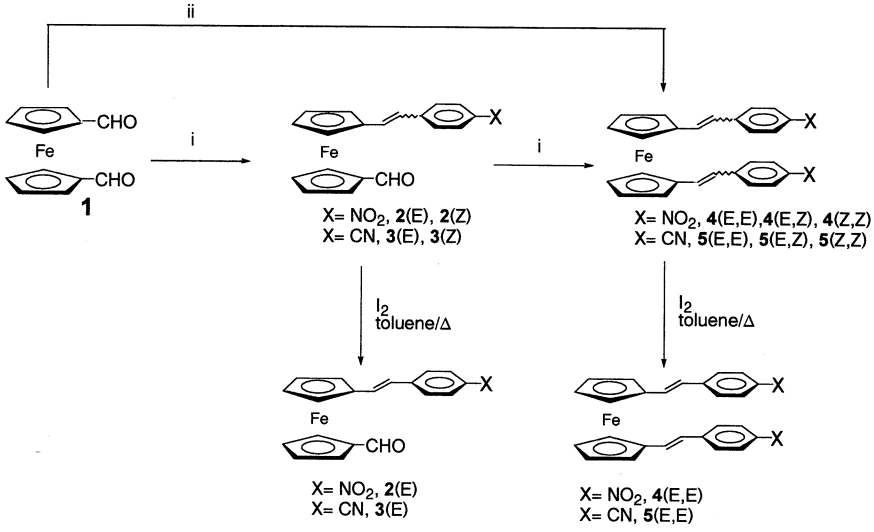

Scheme 2. Syntheses of **2**−**5**. (i) 1.5 ($PPh_3CH_2-C_6H_4$-4-NO_2)Br/KO*t*Bu or 1.5 ($PPh_3CH_2-C_6H_4$-4-CN)Br/KO*t*Bu. (ii) 3 ($PPh_3CH_2-C_6H_4$-4-NO_2)Br/KO*t*Bu, or 3 ($PPh_3CH_2-C_6H_4$-4-CN)Br/KO*t*Bu.

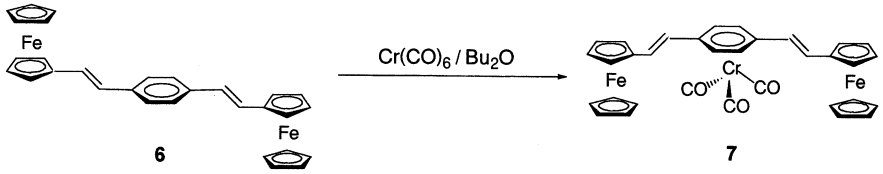

Scheme 3

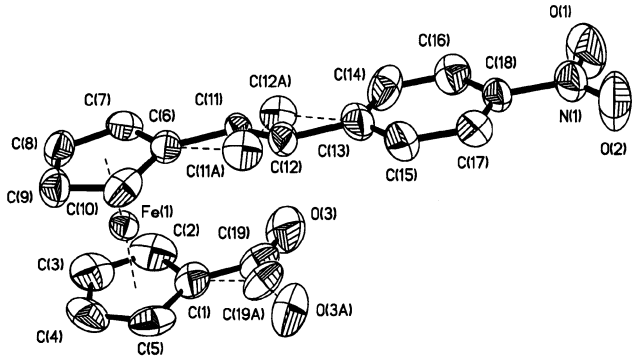

Figure 1. Molecular structure and atomic labeling scheme for **2**-(*E*), Fe(η^5-C_5H_4CHO){η^5-C_5H_4−(*E*)-CH=CHC_6H_4-4-NO_2}, with 50% anisotropic displacement ellipsoids

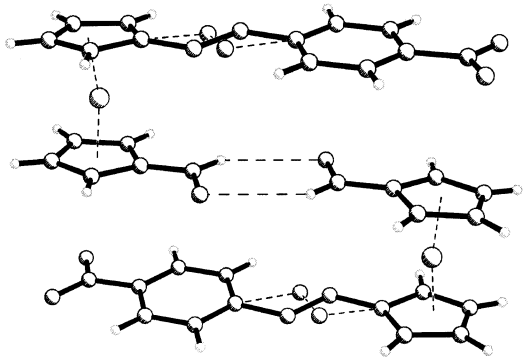

Figure 2. Crystal packing of compound **2**-(*E*) showing the hydrogen-bonding through the aldehydes of two different molecules. The distance between H···O is ca. 2.7 Å

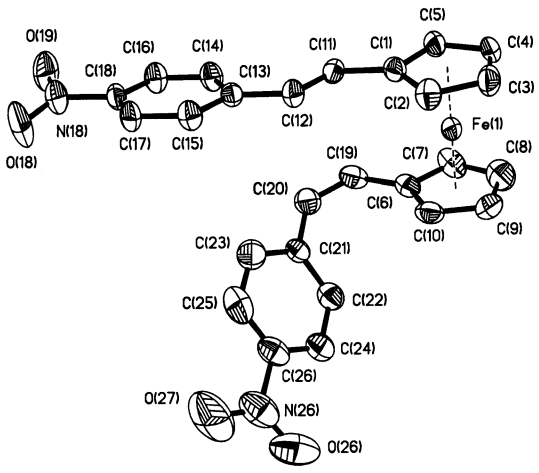

Figure 3. Molecular structure and atomic labeling scheme for **4**-(*E,Z*), Fe{η^5-C_5H_4−(*Z*)-CH=CHC_6H_4-4-NO_2}{η^5-C_5H_4−(*E*)-CH=CHC_6H_4-4-NO_2}, with 50% anisotropic displacement ellipsoids

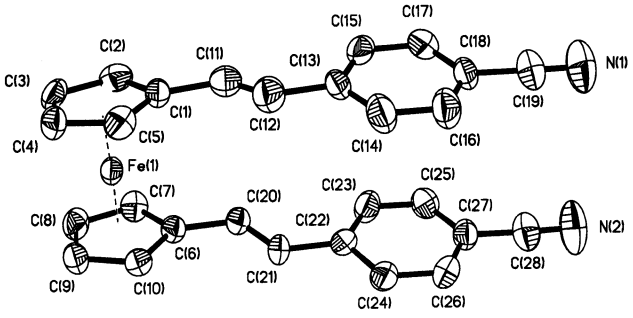

Figure 4. Molecular structure and atomic labeling scheme for **5**-(*E,E*), Fe{η^5-C_5H_4−(*E*)-CH=CHC_6H_4-4-CN}$_2$, with 50% anisotropic displacement ellipsoids

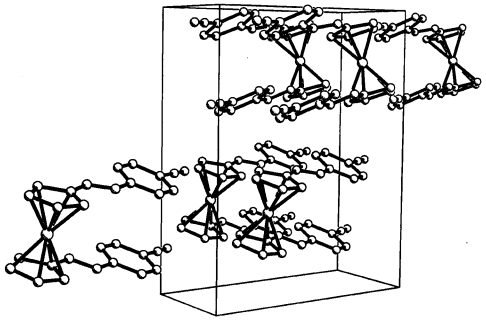

Figure 5. Cell packing diagram for **5**-(*E,E*), Fe{η^5-C_5H_4−(*E*)-CH=CHC_6H_4-4-CN}$_2$

ferrocenyl complexes, it has been reported that two molecular motions relieve steric strain:[1] (i) the rotation from an eclipsed to a staggered disposition of the two Cp rings and (ii) their tilting from a parallel disposition. For these three complexes, little tilting is observed; the two cyclopentadienyl rings are slightly tilted (dihedral angles 2.7−4.3°) with respect to each other. Compounds **2**-(*E*), **4**-(*E,Z*), and **5**-(*E,E*) show *syn* conformations with respect to the two ancillary ligands, with a perfect eclipsed disposition of the Cp rings of the ferrocene unit in **2**-(*E*) and **5**-(*E,E*).

The distances from iron to the cyclopentadienyl rings and the C−C distances within the rings in these three structures, lie in the expected range. As seen in Figures 1, 2, 3, and 4, all the molecules with (*E*) stereochemistry have an almost idealized coplanar arrangement between the ferrocenyl donor and the vinylene-phenylene functionalized fragment. The two ancillary ligands in compound **5**-(*E,E*) show intra-

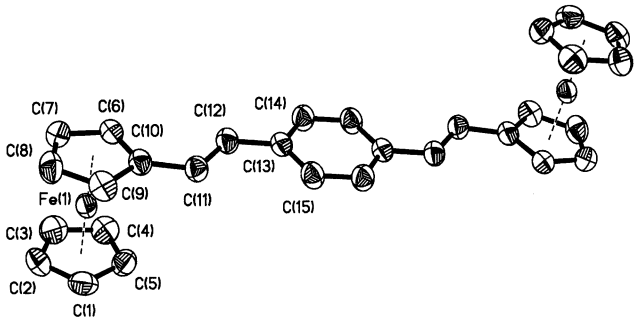

Figure 6. Molecular structure and atomic labeling scheme for **6**, Fe(η^5-C_5H_5)(η^5-C_5H_4−(*E*)-CH=CH−4-C_6H_4−(*E*)-CH=CH−η^5-C_5H_4)Fe(η^5-C_5H_5), with 50% anisotropic displacement ellipsoids

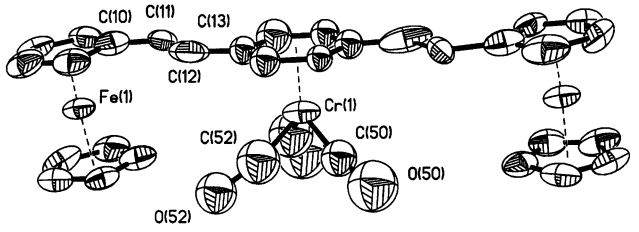

Figure 7. Molecular structure and atomic labeling scheme for **7**, Fe(η^5-C_5H_5)(η^5-C_5H_4−(*E*)-CH=CH−4-{(η^6-C_6H_4)Cr(CO)$_3$}-(*E*)-CH=CH−η^5-C_5H_4)Fe(η^5-C_5H_5) with 50% anisotropic displacement ellipsoids

Table 1. Selected bond lengths and angles for **2**-(*E*), **4**-(*E,Z*), and **5**-(*E,E*)

2-(*E*)			
N1−O1	1.216(3)	Fe1−N1 (space)	9.42
N1−O2	1.212(3)	Fe1−N1 (bonds)	11.9
C19−O3	1.188(10)		
C19A−O3A	1.135(18)		
plane Cp(1−5)−Cp(6−10)		4.28(0.21)	
plane Cp(1−5)−Ph		7.18(0.20)	
4-(*E,Z*)			
N18−O18	1.221(3)	Fe1−N18 (space)	9.41
N18−O19	1.218(4)	Fe1−N26 (space)	7.97
N26−O26	1.225(4)	Fe1−N18 (bonds)	11.90
N26−O27	1.208(4)	Fe1−N26 (bonds)	11.92
plane Cp(1−5)−Cp(6−10)		3.01(0.24)	
plane Cp(1−5)−Ph(13−18)		9.51(0.19)	
5-(*E,E*)			
C11−C20	3.44	Fe1−N1 (space)	10.46
C12−C21	3.71	Fe1−N2 (space)	10.56
C19−C28	3.89	Fe1−N1 (bonds)	13.0
N1−N2	3.92	Fe1−N2 (bonds)	13.0
plane Cp(1−5)−Cp(6−10)		2.75(0.16)	
plane Cp(1−5)−Ph(13−18)		10.93(0.16)	
plane Cp(6−10)−Ph(22−27)		7.57(0.17)	
plane Ph(13−18)−Ph(22−27)		2.30(0.13)	

Table 2. Selected bond lengths and angles for **6** and **7**

	6	**7**
Fe−C (Cp subs.)	2.047[10]	2.024[25]
Fe−C (Cp non subs.)	2.041[1]	2.022[40]
C−C (Cp subs.)	1.417 [10]	1.403[25]
C−C (Cp non subs.)	1.407[5]	1.401[8]
C(10)−C(11)	1.464(2)	1.34(2)
C(11)−C(12)	1.323(2)	1.37(3)
C(12)−C(13)	1.469(2)	1.40(3)
Cr1−C(CO)	−	1.72[9]
C(CO)−O(CO)	−	1.24[10]
Fe−Fe (space)	13.49	12.85
Fe−Fe (bonds)	17.86	16.46
Fe−Cr (space)	−	6.14
Fe−Cr (bonds)	−	8.15
C(10)−C(11)−C(12)	124.59(18)	121(2)
C(11)−C(12)−C(13)	128.02(18)	122(3)
plane Cp−Cp(subs)	1.46(16)	0.29(0.73)
plane Ph−Cp(subs)	3.37(25)	5.03(1.11)

molecular π-stacking, as can be clearly seen in Figure 4; the two ligands smoothly increase their separation from 3.44 [C(20)−C(11)] to 3.92 Å [N(1)−N(2)]. In the crystal lattice of compound **2**-(*E*), centrosymmetric dimer pairs are connected by hydrogen-bonding through the oxygen and hydrogen atoms of the aldehyde group (Figure 2). This hydrogen-bond of the type C−H···O is pervasive in crystalline organometallic transition metal complexes, especially when the C−H is of the sp^2 type.[11] In our case, the oxygen atom of the aldehyde polarizes the C−H bond enhancing its H-donor capabilities. Compound **5**-(*E,E*) crystallizes in the noncentrosymmetric space group $P2_1$. The crystal arrangement of **5**-(*E,E*) (Figure 5), despite being noncentrosymmetric, reveals an anti-parallel alignment of the molecular dipoles, therefore low second-harmonic generation (SHG) is expected for the bulk material. This canceling of the molecular dipoles has also been observed for other noncentrosymmetric ferrocenyl compounds.[12]

Compounds **6** and **7** both crystallize in the centrosymmetric space group $P2_1/c$, the inversion center for compound **6** is located in the middle of the phenyl ring. The crystallographic inversion center lies very close to the chromium atom, generating another molecule with a face to face disposition when compared with the previous one, thus resulting in disorder. The bond lengths and angles in **6** lie in the expected range,[13] with the ferrocenyl units adopting the sterically less hindered *anti* conformation. The cyclopentadienyl and phenyl rings in **6** are roughly coplanar (maximum dihedral angle 3.37°). The bond lengths and angles in **7** lie in the expected range, except the Cr−C−O angles which are significantly distorted from linearity (ca. 167°). The most significant structural feature of **7** is the *syn*/*syn* conformation adopted by the two ferrocenyl and the tri(carbonyl)chromium units. The two substituted-cyclopentadienyl rings and the phenyl group are more distorted from coplanarity (maximum dihedral angle 5.03°) than the similar rings in compound **6**.

The Fe−Cr distances in **7** are 6.1 Å (through space) and 8.2 Å (through bonds), so a direct bonding effect must be discounted. In the absence of conclusive theoretical calculations, we believe that the more sterically hindered disposition of the ligated metal units may be due to packing effects. In fact, this kind of disposition has also been observed in other related compounds.[14]

Cyclic Voltammetry

The electrochemical data obtained for complexes **2**−**5** are summarized in Table 3. In all cases, we observed the chemically reversible ferrocene/ferrocenium couple with $i_{pa}/i_{pc} = 1$. Although the peak to peak separations in all the compounds are greater than the ideal value for a fully reversible one-electron process, this difference ($E_{pc} - E_{pa}$) is similar to that measured for ferrocene under the conditions of the experiment. When compared with the previously reported ferrocenyl derivatives with one 4-nitrophenylethenyl or 4-cyanophenylethenyl substituent,[4−6] the bis-substituted complexes show a more anodic half-wave potential (ca. 100 mV), suggesting that the extra electron-accepting substituent has an important electronic effect on the ferrocenyl fragment. When comparing complexes with analogous stereochemical features, the nitro compounds **4** have a higher oxidation potential than the homologous nitrile derivatives **5**, thus confirming the better electron-accepting nature of the nitro group. The complexes with a higher degree of (*E*) stereochemistry (i.e. *E,E* > *E,Z* > *Z,Z*) possess a lower half-wave potential than those with a higher degree of (*Z*) stereochemistry (half-wave potential **4**-(*E,E*) < **4**-(*E,Z*) < **4**-(*Z,Z*) and **5**-(*E,E*) < **5**-(*E,Z*) < **5**-(*Z,Z*)]. This is in good agreement with the greater stabilization of the positive charge corresponding to the more effective conjugation of the (*E*) isomers, and indicates a higher degree of charge transfer from the metal center to the polyene backbone.[5,6,15] The aldehydes **2** and **3** possess a much higher half-wave potential than the ferrocenyl complexes with one 4-nitrophenylethenyl or 4-cyanophenylethenyl substituent,[4−6] perhaps due to the electron-accepting nature of the aldehyde group. The substitution of the aldehyde group by the corresponding conjugated ligand to give **4** and **5**, results in a shift to more cathodic potentials, probably as a consequence of the enhanced stabilization of the positive charge of the resultant ferrocenium species at the two conjugated ancillary ligands.

Literature electrochemical data suggest that biferrocene complexes similar to **6** and **7** do not show effective electronic communication between the two ferrocene moieties.[8,13] For such complexes, and homologues with pentamethylcyclopentadienyl ligands, only one peak is observed for the oxidation of the iron atoms. However, the potential for this two-electron oxidation is sensitive to modification of the bridging unit; electrochemical data for compound **7** shows that the oxidation of the iron atom is clearly influenced by the carbonyl fragment. A shift from 455 mV in compound **6** to 351 mV in **7** is consistent with oxidation of the ferrocene centers which is facilitated by incorporation of the chromium carbonyl unit.[8] In fact, one would expect that the electron-accepting nature of chromium tricarbonyl should increase the oxidation potential of the compound in contrast to what we observed. The same effect has been described by Müller for compound **7** and other related ferrocenyl-chromium tricarbonyl complexes[8] and, in fact, may be justified by the amphoteric character of $Cr(CO)_3$ proposed by the same author and his co-workers.[16]

Table 3. Electrochemical and linear optical data for complexes **2**−**5**

	λmax (nm)						
	$CHCl_3$		MeOH		THF		$E_{1/2}(\Delta E_p)$/mV
Compd.	MLCT	π-π*	MLCT	π-π*	MLCT	π-π*	(Ferrocene based)[a]
2-(*E*)	−	309	−	356	−	358	755(74)
2-(*Z*)	−	308	−	325	−	329	790(170)
3-(*E*)	−	327	−	329	−	329	775(127)
4-(*E,E*)	494	358	497	358	495	355	545(89)
4-(*E,Z*)	493	350	487	353	488	352	555(74)
4-(*Z,Z*)	481	335	−	337	481	343	585(155)
5-(*E,E*)	−	342	−	340	492	340	500(100)
5-(*E,Z*)	473	334	473	333	469	335	545(115)
5-(*Z,Z*)	−	318	−	312	−	319	565(79)
6							455
7	436[b]	306[b]					351[b]

[a] Ferrocene half-wave potential = 445(105) mV. − [b] Data taken from ref. [8].

Electronic Spectra

Table 3 contains the electronic spectroscopic data for the bis-substituted complexes **2**−**5**. In a typical electronic spectrum of substituted ferrocenyl complexes, two prominent bands are often observed in the range of 500 to 300 nm. The more energetic band (300−360 nm) is assigned to a π−π* intra-ligand transition, and the less energetic band (400−500 nm) is assigned to a metal to ligand charge-transfer band (MLCT). A weak band at higher wavelengths (about 500 nm), assigned to a *d-d* transition, is only discernible in some cases as a shoulder on the MLCT band, and is not shown in Table 3. This assignment is in accordance to the theoretical results reported by Barlow et al. (model III in ref.[17]) and to other experimental results,[5,6,12,18−23] although we are aware that some controversy about this assignment has been reported.[24] The MLCT band is influenced by the nature of the ancillary ligand, showing a hypsochromic shift on increasing the (*E*) character of the complex. The more intense π-π* band shows a similar dependence on the nature of the ligand; this is because the (*E*) stereochemistry promotes a more effective conjugation than the (*Z*) stereochemistry, thus lowering the energy of the π* orbital. Solvatochromism affords an idea of the dipole moments in the ground and in the excited states. These are related to hyperpolarizability, and therefore solvatochromism is a useful indicator for the potential for second-order NLO behavior. The bis-substituted ferrocenyl complexes show moderate solvatochromic behavior across the solvents surveyed.

Kurtz Powder Studies

Kurtz powder measurements were performed on **4**-(*E,Z*), **4**-(*Z,Z*), **4**-(*E,E*), **5**-(*E,Z*), **5**-(*E,E*), **6**, and **7**. Initial studies using ns pulses at 1.064 μm suggested the doubling of the frequency for a number of samples (green flashes were observed when the samples were irradiated), but absorption associated with the MLCT bands in these complexes rendered these results qualitative at best. A second qualitative test at the important telecommunications wavelength of 1.3 μm using fs pulses again suggested the doubling of the frequency (red flashes were observed for most complexes). A third qualitative test at 1.4 μm confirmed this result. Importantly, all complexes are transparent at both the fundamental and second-harmonic frequencies corresponding to the wavelength of 1.3 μm, so the SHG merit of these complexes was quantified against an urea standard, the results for which are summarized in Table 4.

Complexes **4**-(*E,Z*), **4**-(*Z,Z*), and **5**-(*E,Z*) showed a relatively strong emission with a significant blue component; this may be due to other NLO processes, and it masks any SHG which may be present, rendering further discussion of these complexes unwarranted. The ferrocene-containing conjugated compounds **4**-(*E,E*) and **5**-(*E,E*) both gave significant responses. Noncentrosymmetric crystal packing is a requirement for observable SHG, therefore it is worthy to note that the structural study of **5**-(*E,E*) reveals a lack of a center of symmetry in the crystal lattice. Complex **6** shows no observable SHG at 1.3 μm, in contrast to the $Cr(CO)_3$-ligated complex **7**. Both complexes crystallize in the centrosymmetric space group $P2_1/c$. The observed SHG for the centrosymmetric **7** is not unique; similar observations for $[Ru(C{=}CPhN{=}N{-}4\text{-}C_6H_4OMe)(PPh_3)_2(\eta^5\text{-}C_5H_5)]BF_4$[25] and $[(\eta^5\text{-}C_5H_5)(CO)_2Fe(\mu\text{-}CO)\{\mu\text{-}(E)\text{-}CH{=}CH{-}4\text{-}C_6H_4\text{-}NMe_2\}Fe(CO)_2(\eta\text{-}C_5H_5)]BF_4$,[26] both of which pack in centrosymmetric space groups, were assigned to effects originating in the noncentrosymmetric crystal surface, small contributions from a noncentrosymmetric phase, or minor deviations from centrosymmetry. Electron diffraction studies to resolve this ambiguity were similarly inconclusive.

The results of the present series of samples emphasize the challenges inherent in translating significant molecular nonlinearities to useful bulk susceptibilities. Thus, while $Fe(\eta^5\text{-}C_5H_5)(\eta^5\text{-}C_5H_4{-}(Z)\text{-}CH{=}CH{-}4\text{-}C_6H_4NO_2)$ is reported to give SHG with an efficiency 62 times that of urea,[19,26–28] incorporation of a further 4-nitrophenylethenyl group in proceeding to **4**-(*E,Z*) or **4**-(*Z,Z*), results in complexes for which observable SHG could not be determined unambiguously.

Third-Order NLO Studies

Third-order nonlinearities of **4**-(*Z,Z*), **5**-(*E,E*), **6**, and **7** were evaluated by the Z-scan technique at 800 nm;[29] the results of these measurements are given in Table 4. Complex **4**-(*E,E*) was insufficiently soluble, in both dichloromethane and THF, to afford useful data.

Early studies of ferrocenyl complexes by optical power limiting afforded very high nonlinearities (10^{-32} to 10^{-31} esu),[30–32] but this technique is carried out on a ns time scale, and contributions from thermal effects may exist. For structure-activity studies, it is more useful to use Z-scan with fs pulses, as in the present study. The cubic nonlinearities $|\gamma|$ of these new ferrocenyl complexes are of the same magnitude as those of related conjugated ferrocenyl complexes examined by degenerate four-wave mixing (DFWM).[33]

One advantage of Z-scan relative to DFWM is that one can readily determine the real and imaginary components of the cubic hyperpolarizabilities, (these are also listed in Table 4). We have previously used Z-scan to study the cubic hyperpolarizabilities of acetylide complexes,[34–40] for which most real components are large and negative, and imaginary components are large, indicative of significant two-photon dispersion effects. The real components of the nonlinearities γ_r for the present series of complexes are large and positive and, with the exception of **4**-(*E,Z*), the imaginary components γ_i are small; two-photon effects are therefore likely to be minor, permitting cautious comment on the effect of structural variation on cubic NLO merit. Replace-

Table 4. Linear optical and nonlinear optical response parameters for **4**-(*Z,Z*), **4**-(*E,Z*), **4**-(*E,E*), **5**-(*E,Z*), **5**-(*E,E*), **6**, and **7**

Complex	λ_{max} (nm)[a] [ε (10^4 м$^{-1}$ cm^{-1}]	SHG[b] (urea = 1)	γ_r[c] (10^{-36} esu)	γ_i[c] (10^{-36} esu)	$\lvert\gamma\rvert$ (10^{-36} esu)
$Fe\{\eta^5\text{-}C_5H_4\text{-}(E)\text{-}CH{=}CHC_6H_4\text{-}4\text{-}NO_2\}_2$ [**4**-(*E,E*)]	495 [0.47]	0.28	[e]	[e]	[e]
$Fe\{\eta^5\text{-}C_5H_4\text{-}(E)\text{-}CH{=}CHC_6H_4\text{-}4\text{-}NO_2\}$-$\{\eta^5\text{-}C_5H_4\text{-}(Z)\text{-}CH{=}CHC_6H_4\text{-}4\text{-}NO_2\}$ [**4**-(*E,Z*)]	488 [0.56]	[d]	840 ± 400	770 ± 200	1140 ± 430
$Fe\{\eta^5\text{-}C_5H_4\text{-}(Z)\text{-}CH{=}CHC_6H_4\text{-}4\text{-}NO_2\}_2$ [**4**-(*Z,Z*)]	481 [0.30]	[d]	600 ± 300	0 ± 50	600 ± 300
$Fe\{\eta^5\text{-}C_5H_4\text{-}(E)\text{-}CH{=}CHC_6H_4\text{-}4\text{-}CN\}_2$ [**5**-(*E,E*)]	492 [0.34]	0.24	280 ± 150	30 ± 20	280 ± 150
$Fe\{\eta^5\text{-}C_5H_4\text{-}(E)\text{-}CH{=}CHC_6H_4\text{-}4\text{-}CN\}$-$\{\eta^5\text{-}C_5H_4\text{-}(Z)\text{-}CH{=}CHC_6H_4\text{-}4\text{-}CN\}$ [**5**-(*E,Z*)]	469 [0.33]	[d]	310 ± 200	50 ± 30	310 ± 200
$Fe(\eta\text{-}C_5H_5)\{\eta^5\text{-}C_5H_4\text{-}(E)\text{-}CH{=}CH\text{-}4\text{-}C_6H_4\text{-}(E)\text{-}CH{=}CH\text{-}\eta^5\text{-}C_5H_4\}Fe(\eta^5\text{-}C_5H_5)$ (**6**)	457 [0.45]	[d]	640 ± 300	30 ± 20	640 ± 300
$Fe(\eta\text{-}C_5H_5)(\eta^5\text{-}C_5H_4\text{-}(E)\text{-}CH{=}CH\text{-}4\text{-}\{(\eta^6\text{-}C_6H_4)\text{-}Cr(CO)_3\}\text{-}(E)\text{-}CH{=}CH\text{-}\eta^5\text{-}C_5H_4)Fe(\eta^5\text{-}C_5H_5)$ (**7**)	455 [0.31]	0.14	850 ± 300	95 ± 30	860 ± 300

[a] All solution measurements (linear optical spectra, third-order NLO studies) in THF as solvent. All complexes are optically transparent at 1.3 μm and 800 nm. – [b] Bulk second-order responses by the Kurtz powder method at 1.3 μm. – [c] Third-order NLO measurements by Z-scan at 800 nm, referenced to the nonlinear refractive index of silica $n_2 = 3{\cdot}10^{-16}$ cm$^2{\cdot}$W^{-1}. – [d] Not determined unambiguously. – [e]Insufficiently soluble.

ment of CN by NO_2 in proceeding from **5**-(*E,Z*) to **4**-(*E,Z*), leads to a significant increase in both γ_r and $|\gamma|$; increase in acceptor-strength leads to increased quadratic nonlinearity in dipolar organometallic complexes,[10] and a similar increase in cubic nonlinearity for the present complexes on increasing acceptor-strength is not unexpected. Errors do not permit comment on the effect of bridge stereochemistry modification on γ_r and $|\gamma|$. The linked complex **6** has substantial γ_r and $|\gamma|$ values despite the absence of a molecular dipole; a large cubic nonlinearity ($\gamma = 504 \pm 52 \times 10^{-36}$ esu, as measured by DFWM at 0.60 μm) was reported for a complex with this composition in earlier work, although the bridge stereochemistry was not specified.[33] Interestingly, incorporation of the bridge-ligated $Cr(CO)_3$ unit in proceeding from **6** to **7**, results in an increase in both γ_r and $|\gamma|$. Recent studies concluded that the $Cr(CO)_3$ unit behaves as an electronically amphoteric auxochrome in chromium carbonyl arene complexes with conjugated side-chains,[16] resulting in significant quadratic nonlinearities for complexes with donor- or acceptor- substituents on the side-chain. In the present system, complex **6** has a donor-bridge-donor composition, whereas our electrochemistry studies suggest that **7** has a donor-donor-donor composition; the increase in the ease of oxidation in proceeding from **6** to **7** probably correlates with an increase in the ease of polarization of electron density, and may be responsible for the increased cubic nonlinearity.

Experimental Section

General Remarks: All reactions were carried out under a nitrogen atmosphere using standard Schlenk techniques. Solvents for synthesis and electrochemical measurements were dried and deoxygenated by standard methods before use. Chromatographic work was performed on silica gel 60 Å or neutral alumina columns.

NMR spectra were recorded on Varian Innova 300 MHz and 500 MHz spectrometers, using $CDCl_3$ as solvent unless otherwise stated. − IR spectra were recorded on a Perkin−Elmer System 2000 FT-IR using NaCl pellets. − Electronic absorption spectra were obtained on a UV-1603 Shimadzu spectrophotometer. − Elemental analyses were performed on a EA 1108 CHNS-O Carlo Erba instrument. − Cyclic voltammetry experiments were performed with a Echochemie pgstat 20 electrochemical analyzer. All measurements were carried out at room temperature with a conventional three-electrode configuration consisting of platinum working and auxiliary electrodes and a Ag/AgCl reference electrode containing aqueous 3 M KCl. The solvent used in all experiments was CH_2Cl_2, which was obtained in HPLC grade and used as received. The supporting electrolyte was 0.1 M tetra-*n*-butylammonium hexafluorophosphate, synthesized by reaction of tetra-*n*-butylammonium bromide and HPF_6, recrystallized from ethanol and dried under vacuum. $E_{1/2}$ values were determined as $(E_{p,a} + E_{p,c})/2$, where $E_{p,a}$ and $E_{p,c}$ are the anodic and cathodic peak potentials, respectively. All reported potentials are not corrected for the junction potential. − Electrospray mass spectra were recorded using a Micromass Quattro LC instrument, using CH_3CN and/or CH_3OH as the mobile phase solvent. The samples were added to give a mobile phase with an approximate concentration of 0.1 mM. This solution was injected into the spectrometer via a Rheodyne injector fitted with a 10 μL sample loop, and nitrogen was employed as a drying and nebulizing gas. − $Fe(\eta^5\text{-}C_5H_5)(\eta^5\text{-}C_5H_4\text{-}(E)\text{-}CH{=}CH\text{-}4\text{-}C_6H_4\text{-}(E)\text{-}CH{=}CH\text{-}\eta^5\text{-}C_5H_4)Fe(\eta^5\text{-}C_5H_5)$ (**6**) was synthesized by literature procedures.[41,42]

1. Preparation of (*E*)- and (*Z*)-Fe(η⁵-C₅H₄CHO)(η⁵-C₅H₄CH=CH−C₆H₄-4-NO₂) (2) and (*E*)-and (*Z*)-Fe(η⁵-C₅H₄CHO)(η⁵-C₅H₄CH=CH−C₆H₄-4-CN) (3): Potassium *tert*-butoxide (258 mg, 2.3 mmol) was added to a solution of 4-nitrobenzyltriphenylphosphonium bromide (988 mg, 2.1 mmol), or 4-cyanobenzyltriphenylphosphonium bromide (963 mg, 2.1 mmol) in THF (100 mL) at 0 °C, and the resulting suspension was allowed to warm to room temperature. After 30 min, the yellow-orange suspension indicated that the ylide was completely formed. 1,1′-Ferrocenebis(carboxaldehyde), **1** (500 mg, 2.1 mmol), was then added at 0 °C and the solution was stirred for ca. 15 h at room temperature. After removing the solvent under reduced pressure, the product was separated with a $CH_2Cl_2/H_2O/NaHCO_3$ mixture and the dichloromethane extract dried with $MgSO_4$. Purification by column chromatography on silica gel using hexane/CH_2Cl_2 (3:7) as the eluent afforded pure **2**-(*E*), **2**-(*Z*), **3**-(*E*), and **3**-(*Z*), although **3**-(*Z*) was obtained in such a low yield that only spectroscopic characterization could be achieved.

Compound 2-(*E*), Fe(η⁵-C₅H₄CHO){η⁵-C₅H₄−(*E*)-CH=CH−C₆H₄-4-NO₂}: Yield 35%. − ^{1}H NMR (500 MHz, $CDCl_3$): δ = 9.90 (s, 1 H, CHO); 8.20 (d, 2 H, $^3J_{H\text{-}H}$ = 8.4 Hz, C_6H_4); 7.56 (d, 2 H, $^3J_{H\text{-}H}$ = 8.1 Hz, C_6H_4); 6.96 (d, 1 H, $^3J_{H\text{-}H}$ = 16.2 Hz, CH=CH); 6.76 (d, 1 H, $^3J_{H\text{-}H}$ = 15.9 Hz, CH=CH); 4.78 (s, 2 H, C_5H_4); 4.62 (s, 2 H, C_5H_4); 4.58 (s, 2 H, C_5H_4); 4.46 (s, 2 H, C_5H_4). − ^{13}C NMR (500 MHz, $CDCl_3$): δ = 69.4, 71.5, 71.9, 75.0 (8 C, C_5H_4); 80.6, 84.3 (2 Cq, C_5H_4); 124.8, 126.2, 126.9, 131.2 (6 C, CH=CH and C_6H_4); 144.3, 146.9 (2 Cq, C_6H_4); 194.1 (1 C, CHO). − $C_{19}H_{15}FeNO_3$ (361.18): calcd. C 63.20, H 4.19, N 3.88; found C 63.53, H 4.27, N 3.80.

Compound 2-(*Z*), Fe(η⁵-C₅H₄CHO){η⁵-C₅H₄−(*Z*)-CH=CH−C₆H₄-4-NO₂}: Yield 17%. − ^{1}H NMR (500 MHz, $CDCl_3$): δ = 9.87 (s, 1 H, CHO); 8.14 (d, 2 H, $^3J_{H\text{-}H}$ = 8.5 Hz, C_6H_4); 7.43 (d, 2 H, $^3J_{H\text{-}H}$ = 8.0 Hz, C_6H_4); 6.55 (d, 1 H, $^3J_{H\text{-}H}$ = 12.0 Hz, CH=CH); 6.39 (d, 1 H, $^3J_{H\text{-}H}$ = 12.0 Hz, CH=CH); 4.74 (s, 2 H, C_5H_4); 4.54 (s, 2 H, C_5H_4); 4.31 (s, 2 H, C_5H_4); 4.23 (s, 2 H, C_5H_4). − ^{13}C NMR (500 MHz, $CDCl_3$): δ = 71.3, 71.4, 71.5, 75.0 (8 C, C_5H_4); 81.1, 83.0 (2 Cq, C_5H_4); 124.2, 127.4, 130.1, 130.4 (6 C, CH=CH and C_6H_4); 145.2, 147.2 (2 Cq, C_6H_4); 193.8 (1 C, CHO). − $C_{19}H_{15}FeNO_3$ (361.18): calcd. C 63.20, H 4.19, N 3.88; found C 63.01, H 4.07, N 3.79.

Compound 3-(*E*), Fe(η⁵-C₅H₄CHO){η⁵-C₅H₄−(*E*)-CH=CH−C₆H₄-4-CN}: Yield 40%. − ^{1}H NMR (500 MHz, $CDCl_3$): δ = 9.90 (s, 1 H, CHO); 7.62 (d, 2 H, $^3J_{H\text{-}H}$ = 7.5 Hz, C_6H_4); 7.52 (d, 2 H, $^3J_{H\text{-}H}$ = 8.0 Hz, C_6H_4); 6.89 (d, 1 H, $^3J_{H\text{-}H}$ = 16.0 Hz, CH=CH); 6.72 (d, 1 H, $^3J_{H\text{-}H}$ = 16.0 Hz, CH=CH); 4.79 (s, 2 H, C_5H_4); 4.60 (s, 2 H, C_5H_4); 4.58 (s, 2 H, C_5H_4); 4.44 (s, 2 H, C_5H_4). − ^{13}C NMR (500 MHz, $CDCl_3$): δ = 69.3, 71.5, 71.7, 74.9 (8 C, C_5H_4); 80.7, 84.6 (2 Cq, C_5H_4); 110.9 (1 C, CN); 126.8, 127.1, 130.1, 133.3 (6 C, CH=CH and C_6H_4); 119.8, 142.4 (2 Cq, C_6H_4); 194.2 (1 C, CHO). − $C_{20}H_{15}FeNO$ (341.19): calcd. C 70.43, H 4.43, N 4.11; found C 70.12, H 4.17, N 4.25. − Electrospray MS. Cone 60 V. *m/z* (fragment): 364 [M^+ + Na].

Compound 3-(*Z*), Fe(η⁵-C₅H₄CHO){η⁵-C₅H₄−(*Z*)-CH=CH−C₆H₄-4-CN}: ^{1}H NMR (300 MHz, $CDCl_3$): δ = 9.86 (s, 1 H, CHO); 7.56 (d, 2 H, $^3J_{H\text{-}H}$ = 8.1 Hz, C_6H_4); 7.38 (d, 2 H, $^3J_{H\text{-}H}$ = 8.4 Hz, C_6H_4); 6.50 (d, 1 H, $^3J_{H\text{-}H}$ = 12.0 Hz, CH=CH); 6.33 (d, 1 H, $^3J_{H\text{-}H}$ = 12.0 Hz, CH=CH); 4.73 (t, 2 H, $^3J_{H\text{-}H}$ = 1.8 Hz, C_5H_4);

4.54 (t, 2 H, $^3J_{H-H}$ = 1.8 Hz, C_5H_4); 4.30 (t, 2 H, $^3J_{H-H}$ = 1.8 Hz, C_5H_4); 4.22 (t, 2 H, $^3J_{H-H}$ = 1.8 Hz, C_5H_4).

2. Preparation of (*E,E*)-, (*E,Z*)-, and (*Z,Z*)-Fe{η^5-C_5H_4CH=CHC_6H_4-4-NO_2)$_2$ (4) and (*E,E*)-, (*E,Z*)-, and (*Z,Z*)-Fe{η^5-C_5H_4CH=CHC_6H_4-4-CN}$_2$ (5): These compounds were prepared by two different procedures.

(i) Potassium *tert*-butoxide (202 mg, 1.8 mmol) was added to a solution of 4-nitrobenzyltriphenylphosphonium bromide (706 mg, 1.5 mmol), or 4-cyanobenzyltriphenylphosphonium bromide (688 mg, 1.5 mmol) in THF (100 mL) at 0 °C, and the resulting suspension was allowed to warm to room temperature. After 30 min, the yellow-orange suspension indicated that the ylide was completely formed. Compound **2** or **3** (1.0 mmol) was then added at 0 °C and the solution was stirred for ca. 15 h at room temperature. After removing the solvent under reduced pressure, the product was separated with a CH_2Cl_2/H_2O/$NaHCO_3$ mixture, and the CH_2Cl_2 extract dried with $MgSO_4$. Purification by column chromatography on silica gel using hexane/CH_2Cl_2 (6:4) as the eluent afforded pure compounds **4**-(*E,Z*), **4**-(*Z,Z*), **4**-(*E,E*), **5**-(*E,Z*), **5**-(*Z,Z*), and **5**-(*E,E*).

(ii) Following the same general method described for compounds **2** and **3**, but using a threefold (3.0 mmol) excess of the phosphonium salt with 1.0 mmol Fe(η^5-$C_5H_4CHO)_2$ (**1**), afforded the complexes in higher yields.

Compound 4-(*E,Z*), Fe{η^5-C_5H_4−(*Z*)-CH=CHC_6H_4-4-NO_2}{η^5-C_5H_4−(*E*)-CH=CHC_6H_4-4-NO_2}: Yield 25%. − ^{1}H NMR (500 MHz, $CDCl_3$): δ = 8.21 (d, 2 H, $^3J_{H-H}$ = 8.5 Hz, C_6H_4); 8.07 (d, 2 H, $^3J_{H-H}$ = 8.5 Hz, C_6H_4); 7.53 (d, 2 H, $^3J_{H-H}$ = 8.5 Hz, C_6H_4); 7.38 (d, 2 H, $^3J_{H-H}$ = 8.0 Hz, C_6H_4); 6.98 (d, 1 H, $^3J_{H-H}$ = 16.0 Hz, CH=CH); 6.70 (d, 1 H, $^3J_{H-H}$ = 16.0 Hz, CH=CH); 6.40 (d, 1 H, $^3J_{H-H}$ = 11.5 Hz, CH=CH); 6.37 (d, 1 H, $^3J_{H-H}$ = 12.5 Hz, CH=CH); 4.48 (s, 2 H, C_5H_4); 4.34 (s, 2 H, C_5H_4); 4.24 (s, 2 H, C_5H_4); 4.18 (s, 2 H, C_5H_4). − ^{13}C NMR (500 MHz, $CDCl_3$): δ = 69.5, 71.4, 71.5, 72.0 (8 C, C_5H_4); 82.0, 83.5 (2 Cq, C_5H_4); 124.2, 124.9, 126.3, 126.6, 129.9, 132.0, 132.7 (12 C, CH=CH and C_6H_4); 144.8, 145.5, 146.9 (4 Cq, C_6H_4). − $C_{26}H_{20}FeN_2O_4$ (480.30): calcd. C 65.00, H 4.20, N 5.83; found C 65.12, H 4.07, N 5.89. − Electrospray MS. Cone 25 V. *m/z* (fragment): 503 [M^+ + Na].

Compound 4-(*Z,Z*), Fe{η^5-C_5H_4−(*Z*)-CH=CHC_6H_4-4-NO_2}$_2$: Yield 10%. − ^{1}H NMR (300 MHz, $CDCl_3$): δ = 8.13 (d, 4 H, $^3J_{H-H}$ = 8.7 Hz, C_6H_4); 7.46 (d, 4 H, $^3J_{H-H}$ = 8.4 Hz, C_6H_4); 6.47 (d, 2 H, $^3J_{H-H}$ = 12.0 Hz, CH=CH); 6.39 (d, 2 H, $^3J_{H-H}$ = 11.5 Hz, CH=CH); 4.20 (s, 4 H, C_5H_4); 4.10 (s, 4 H, C_5H_4). − ^{13}C NMR (300 MHz, $CDCl_3$): δ = 71.4, 71.5 (8 C, C_5H_4); 81.9 (2 Cq, C_5H_4); 124.1, 125.8, 130.0, 131.8 (12 C, CH=CH and C_6H_4); 145.5, 146.8 (4 Cq, C_6H_4). − $C_{26}H_{20}FeN_2O_4$ (480.30): calcd. C 65.00, H 4.20, N 5.83; found C 65.23, H 4.37, N 5.92. − Electrospray MS. Cone 40 V. *m/z* (fragment): 503 [M^+ + Na].

Compound 4-(*E,E*), Fe{η^5-C_5H_4−(*E*)-CH=CHC_6H_4-4-NO_2}$_2$: Yield 34%. − ^{1}H NMR (300 MHz, $CDCl_3$): δ = 8.20 (d, 4 H, $^3J_{H-H}$ = 8.7 Hz, C_6H_4); 7.56 (d, 4 H, $^3J_{H-H}$ = 8.4 Hz, C_6H_4); 7.11 (d, 2 H, $^3J_{H-H}$ = 16.2 Hz, CH=CH); 6.79 (d, 2 H, $^3J_{H-H}$ = 16.2 Hz, CH=CH); 4.62 (s, 4 H, C_5H_4); 4.49 (s, 4 H, C_5H_4). − ^{13}C NMR (300 MHz, $CDCl_3$): δ = 71.6, 72.0 (8 C, C_5H_4); 82.3 (2 Cq, C_5H_4); 124.5, 124.9, 127.0, 128.2 (12 C, CH=CH and C_6H_4); 143.5, 144.7 (4 Cq, C_6H_4). Yield 34%. − $C_{26}H_{20}FeN_2O_4$ (480.30): calcd. C 65.00, H 4.20, N 5.83; found C 64.92, H 4.32, N 5.75. − Electrospray MS. Cone 40 V. *m/z* (fragment): 503 [M^+ + Na].

Compound 5-(*E,Z*), Fe{η^5-C_5H_4−(*Z*)-CH=CHC_6H_4-4-CN}{η^5-C_5H_4−(*E*)-CH=CHC_6H_4-4-CN}: Yield 27%. − ^{1}H NMR (300 MHz, $CDCl_3$): δ = 7.62 (d, 2 H, $^3J_{H-H}$ = 8.1 Hz, C_6H_4); 7.48 (m, 4 H, C_6H_4); 7.32 (d, 2 H, $^3J_{H-H}$ = 8.4 Hz, C_6H_4); 6.91 (d, 1 H, $^3J_{H-H}$ = 15.9 Hz, CH=CH); 6.61 (d, 1 H, $^3J_{H-H}$ = 16.2 Hz, CH=CH); 6.31 (s, 2 H, CH=CH); 4.48 (s, 2 H, C_5H_4); 4.34 (s, 2 H, C_5H_4); 4.24 (s, 2 H, C_5H_4); 4.17 (s, 2 H, C_5H_4). − ^{13}C NMR (500 MHz, $CDCl_3$): δ = 69.5, 71.4, 71.7, 72.1 (8 C, C_5H_4); 82.6, 84.3 (2 Cq, C_5H_4); 110.6, 110.8 (2 C, CN); 125.5, 126.8, 129.9, 131.3, 131.5, 132.6, 133.2 (12 C, CH=CH and C_6H_4); 119.7, 119.8, 142.8, 143.4 (4 Cq, C_6H_4). − $C_{28}H_{20}FeN_2$ (440.33): calcd. C 76.42, H 4.58, N 6.36; found C 76.02, H 4.75, N 6.39. − Electrospray MS. Cone 45 V. *m/z* (fragment): 463 [M^+ + Na].

Compound 5-(*Z,Z*), Fe{η^5-C_5H_4−(*Z*)-CH=CHC_6H_4-4-CN}$_2$: Yield 10%. − ^{1}H NMR (300 MHz, $CDCl_3$): δ = 7.54 (d, 4 H, $^3J_{H-H}$ = 7.8 Hz, C_6H_4); 7.39 (d, 4 H, $^3J_{H-H}$ = 7.5 Hz, C_6H_4); 6.42 (d, 2 H, $^3J_{H-H}$ = 11.7 Hz, CH=CH); 6.32 (d, 2 H, $^3J_{H-H}$ = 11.7 Hz, CH=CH); 4.17 (s, 4 H, C_5H_4); 4.06 (s, 4 H, C_5H_4). − ^{13}C NMR (300 MHz, $CDCl_3$): δ = 71.3, 71.5 (8 C, C_5H_4); 82.1 (2 Cq, C_5H_4); 110.7 (2 C, CN); 126.2, 129.9, 131.1, 132.5 (12 C, CH=CH and C_6H_4); 119.7, 143.4 (4 Cq, C_6H_4). − $C_{28}H_{20}FeN_2$ (440.33): calcd. C 76.42, H 4.58, N 6.36; found C 76.55, H 4.26, N 6.20. − Electrospray MS. Cone 45 V. *m/z* (fragment): 463 [M^+ + Na].

Compound 5-(*E,E*), Fe{η^5-C_5H_4−(*E*)-CH=CHC_6H_4-4-CN}$_2$: Yield 36%. − ^{1}H NMR (300 MHz, $CDCl_3$): δ = 7.48 (d, 4 H, $^3J_{H-H}$ = 7.5 Hz, C_6H_4); 7.28 (d, 4 H, $^3J_{H-H}$ = 8.1 Hz, C_6H_4); 6.83 (d, 2 H, $^3J_{H-H}$ = 15.9 Hz, CH=CH); 6.53 (d, 2 H, $^3J_{H-H}$ = 15.9 Hz, CH=CH); 4.48 (s, 4 H, C_5H_4); 4.36 (s, 4 H, C_5H_4). − ^{13}C NMR (300 MHz, $CDCl_3$): δ = 69.2, 71.7 (8 C, C_5H_4); 83.8 (2 Cq, C_5H_4); 110.4 (2 C, CN); 125.4, 126.6, 130.9, 133.1 (12 C, CH=CH and C_6H_4); 119.7, 142.6 (4 Cq, C_6H_4). − $C_{28}H_{20}FeN_2$ (440.33): calcd. C 76.42, H 4.58, N 6.36; found C 76.36, H 4.63, N 6.27. − Electrospray MS. Cone 45 V. *m/z* (fragment): 463 [M^+ + Na].

3. Isomerization Reactions: Compounds **4**-(*E,Z*), **4**-(*Z,Z*), **5**-(*E,Z*), or **5**-(*Z,Z*) could be isomerized to the all-(*E*) complexes by the following method. **4**-(*E,Z*) (300 mg) (or any of the other complexes), was dissolved in 10 mL of toluene with I_2 (10 mg). The mixture was refluxed for 20 minutes, after which the solvent was eliminated by reduced pressure. The crude product was flash-chromatographed, yielding pure **4**-(*E,E*) compound. Yield 85%. Yields for **4**-(*Z,Z*), **5**-(*E,Z*), or **5**-(*Z,Z*) in the range 80−90%.

4. Preparation of Fe(η^5-C_5H_5)(η^5-C_5H_4−(*E*)-CH=CH−4-{(η^6-C_6H_4)Cr$(CO)_3$}-(*E*)-CH=CH−η^5-C_5H_4)Fe(η^5-C_5H_5) (7): $Cr(CO)_6$ (660.2 mg, 3.0 mmol) was added to a solution of compound **6** (300 mg, 0.6 mmol) in butyl ether (40 mL), and the resulting solution stirred for 15 h at 150 °C. After cooling the mixture to room temperature, the solution was filtered and the solvent removed under reduced pressure. Purification by column chromatography on alumina with CH_2Cl_2/hexane (1:1) as the eluent afforded pure **7**, yield 65%.

X-ray Diffraction Studies: Single crystals were grown by slow diffusion of hexane into concentrated CH_2Cl_2 solutions and mounted on a glass fiber in a random orientation. Data collection was performed at room temperature on a Siemens Smart CCD diffractometer using graphite monochromated Mo-K_α radiation (λ = 0.71073 Å) with a nominal crystal to detector distance of 4.0 cm. A hemisphere of data was collected based on three ω-scan runs (starting ω = −28°) at values φ = 0°, 90°, and 180° with the detector at 2θ = 28°. At each of these runs, frames (606, 435, and 230, respectively) were collected at 0.3° intervals and 20 s per frame for compound **2**-(*E*), 40 s per frame for compound **4**-(*E,Z*), 45 s per frame for compound **5**-(*E,E*), 10 s per frame for **6** and 80 s per frame for **7**. The diffraction frames were integrated using the

Table 5. Crystallographic Data

Compound	**2**-(E)	**4**-(*E*,Z)	**5**-(*E*,E)	**6**	**7**
Empirical formula	$C_{19}H_{15}FeNO_3$	$C_{26}H_{20}FeN_2O_4$	$C_{28}H_{20}FeNFeN_2$	$C_{30}H_{26}Fe_2$	$C_{33}H_{26}Fe_2CrO_3$
Molecular weight [g·mol^{-1}]	361.17	480.29	440.31	498.21	634.24
Temperature [K]	293(2)	293(2)	293(2)	293(2)	293(2)
Wavelength [Å]	0.71073	0.71073	0.71073	0.71073	0.71073
Crystal System	Monoclinic	Triclinic	Monoclinic	Monoclinic	Monoclinic
Space group	$P2_1/n$	$P\bar{1}$	$P2_1$	$P2_1/c$	$P2_1/c$
a [Å]	7.6532(5)	7.5874(17)	6.2114(4)	12.7324(4)	17.131(3)
b [Å]	7.6518(5)	10.569(2)	14.0877(8)	7.7128(2)	7.4568(13)
c [Å]	26.6880(17)	14.416(3)	12.1250(7)	11.6266(5)	10.7432(19)
α [deg.]	90	100.919(5)	90	90	90
β [deg.]	91.328(2)	103.232(5)	102.3550(10)	98.5460(10)	99.780(4)
γ [deg.]	90	101.555(6)	90	90	90
Volume [Å^3]	1562.45(18)	1068.5(4)	1036.42(11)	1129.08(7)	1352.4(4)
Z	4	2	2	2	2
Density [calcd. Mg·m^{-3}]	1.535	1.493	1.411	1.465	1.557
Absorption Coef. [mm^{-1}]	0.982	0.743	0.746	1.300	1.487
F(000)	744	496	456	516	648
Crystal Size [mm^3]	0.28×0.23×0.16	0.26×0.11×0.10	0.49×0.44×0.02	0.46×0.14×0.03	0.046×0.042×0.011
θ range [deg.]	1.53 to 30.55	1.50 to 30.59	1.72 to 30.53	1.62 to 30.85	1.21 to 24.70
Index Ranges	$-9 \le h \le 10$	$-8 \le h \le 10$	$-8 \le h \le 8$	$-18 \le h \le 17$	$-11 \le h \le 11$
	$-10 \le k \le 10$	$-15 \le k \le 14$	$-18 \le k \le 20$	$-11 \le k \le 11$	$-7 \le k \le 7$
	$-37 \le l \le 25$	$-20 \le l \le 15$	$-16 \le l \le 17$	$-16 \le l \le 16$	$-7 \le l \le 12$
Reflections Collected	12775	9110	8466	12797	4327
Independent Reflections	4766 [*R*(int.) = 0.0617]	6400 [*R*(int.) = 0.0553]	4917 [*R*(int.) = 0.0313]	3395 [*R*(int.) = 0.0439]	1353 [*R*(int.) = 0.0790]
Data/Restrains/Parameters	4766/0/245	6400/0/298	4917/1/281	3395/0/145	1353/0/182
Goodness-of-fit-on F^2	0.868	0.844	0.876	0.916	1.082
Final *R* indices [$I > 2\sigma(I)$]	*R*1=0.0454, *wR*2=0.0850	*R*1=0.0572, *wR*2=0.0943	*R*1=0.0422, *wR*2=0.0720	*R*1=0.0328, *wR*2=0.0669	*R*1=0.0699, *wR*2=0.1749
R indices (all data)	*R*1=0.1366, wR2=0.1027	*R*1=0.1679, *wR*2=0.1191	*R*1=0.0867, *wR*2=0.0805	*R*1=0.0748, *wR*2=0.0760	*R*1=0.1034, *wR*2=0.2006
ρ max, ρ min. [e Å^{-3}]	0.529, −0.261	0.758, −0.599	0.428, −0.246	0.303, −0.229	0.456, −0.507

SAINT package and corrected for absorption with SADABS.[43,44] Space group assignments are based on systematic absences, E statistics, and successful refinement of the structures. Structures were solved by direct methods with the aid of successive difference Fourier maps and were refined using the SHELXTL 5.1 software package. All non-hydrogen atoms were refined anisotropically. Hydrogen atoms were assigned to ideal positions and refined using a riding model. Data collection parameters are given in Table 5.

Kurtz Powder Studies: Samples were ungraded powders placed in the circular cavity (10 mm diameter × 0.5 mm depth) of a microscope slide with a cover slip. Powder SHG efficiencies were measured using the Kurtz technique.[45] Studies utilizing the fundamental output of a Q-switched Quanta-Ray GC-130 Nd:YAG laser (1.06 μm) were inconclusive due to material resonances at the second-harmonic frequency. The powder measurements were therefore performed at 1.3 and 1.4 μm using a Light Conversion Topas optical parametric generator pumped with a Clark MXR regenerative amplifier. This afforded approximately 150 fs pulses at a 1 kHz repetition rate which were directed onto the sample as an unfocussed beam (spot size about 5 mm; energy per pulse: up to 20 mJ). The intensity of the generated powder SHG was determined using a Coolsnap Photometric CCD camera. Measurements thus made were compared with those of a urea powder sample.

Z-scan Measurements: Z-scan measurements were performed at 800 nm using 100 fs pulses from a system consisting of a Coherent Mira Ti-sapphire laser pumped with a Coherent Innova or Coherent Verdi cw pump and a Ti-sapphire regenerative amplifier pumped with a frequency-doubled Q-switched pulsed YAG laser (Spectra Physics GCR) at 30 Hz and employing chirped pulse amplification. Tetrahydrofuran solutions were examined in a glass cell with a 0.1 cm path length. The Z-scans were recorded at three concentrations for each compound [two concentrations for **4**-(*E,E*), **4**-(*Z,Z*), and **5**-(*E,E*)] and the real and imaginary part of the nonlinear phase change determined by numerical fitting.[29] The real and imaginary part of the hyperpolarizability of the solute was then calculated assuming linear concentration dependencies of the nonlinear phase shifts. The nonlinearities and light intensities were calibrated using measurements of a 1 mm thick silica plate for which the nonlinear refractive index $n_2 = 3 \cdot 10^{-16}$ cm^2·W^{-1} was assumed.

Supplementary Data: Crystallographic data (excluding structure factors) for the structures reported in this paper have been deposited with the Cambridge Crystallographic Data Centre as supplementary publication no. CCDC-152432 for compound **2**-(*E*), CCDC-152433 for compound **4**-(*E,Z*), CCDC-152434 for compound **5**-(*E,E*), CCDC-152435 for compound **6**, and CCDC-152436 for compound **7**. Copies of the data can be obtained free of charge on application to CCDC, 12 Union Road, Cambridge CB2 1EZ, UK. [Fax: (internat.) +44−1223/336-033; E-mail: deposit@ccdc.cam.ac.uk].

Acknowledgments

We thank the DGESIC (PB98-1044), BANCAIXA (P1B98-07) and the Australian Research Council (ARC) for financial support. J. A. M. thanks the Generalitat Valenciana for a fellowship, and MGH thanks the ARC for a Senior Research Fellowship.

[1] A. Togni, T. Hayashi, *Ferrocenes: Homogeneous Catalysis-Organic Synthesis Materials-Science*, VCH Publishers, New York, NY (USA) **1995**.
[2] A. Togni, R. L. Halterman, *Metallocenes*, Wiley-VCH, Weinheim (Germany), **1998**.
[3] N. J. Long, *Metallocenes*, Blackwell Science, London, **1997**.
[4] J. Mata, S. Uriel, E. Peris, R. Llusar, S. Houbrechts, A. Persoons, *J. Organomet. Chem.* **1998**, *562*, 197.
[5] J. A. Mata, E. Falomir, R. Llusar, E. Peris, *J. Organomet. Chem.* **2000**, *616*, 80.

[6] J. A. Mata, S. Uriel, R. Llusar, E. Peris, *Organometallics* **2000**, *19*, 3797.
[7] I. S. Lee, Y. K. Chung, J. Mun, C. S. Yoon, *Organometallics* **2000**, *18*, 5080.
[8] T. J. J. Müller, *J. Organomet. Chem.* **1999**, *578*, 95.
[9] I. R. Whittall, A. M. McDonagh, M. G. Humphrey, M. Samoc, *Adv. Organomet. Chem. Vol 43*, Academic Press Inc, San Diego, **1999**, p. 349.
[10] I. R. Whittall, A. M. McDonagh, M. G. Humphrey, M. Samoc, *Adv. Organomet. Chem. Vol 42*, Academic Press Inc, San Diego, **1998**, p. 291.
[11] D. Braga, F. Grepioni, G. R. Desiraju, *Chem. Rev.* **1998**, *98*, 1375.
[12] A. Houlton, J. R. Miller, J. Silver, N. Jassim, M. J. Ahmet, T. L. Axon, D. Bloor, G. H. Cross, *Inorg. Chim. Acta* **1993**, *205*, 67.
[13] A. Hradsky, B. Bildstein, N. Schuler, H. Schottenberg, P. Jaitner, K.-H. Ongania, K. Wurst, J.-P. Launay, *Organometallics* **1997**, *16*, 392.
[14] P. A. Deck, M. J. Lane, J. L. Montgomery, C. Sebodnick, *Organometallics* **2000**, *19*, 1013.
[15] D. Naskar, S. K. Das, L. Giribabu, B. G. Maiya, S. Roy, *Organometallics* **2000**, *19*, 1464.
[16] T. J. J. Müller, A. Netz, M. Ansorge, E. Schmalzlin, C. Brauchle, K. Meerholz, *Organometallics* **1999**, *18*, 5066.
[17] S. Barlow, H. E. Bunting, C. Ringham, J. C. Green, G. U. Bublitz, S. G. Boxer, J. W. Perry, S. R. Marder, *J. Am. Chem. Soc.* **1999**, *121*, 3715.
[18] J. C. Calabrese, L.-T. Cheng, J. C. Green, S. R. Marder, W. Tam, *J. Am. Chem. Soc.* **1991**, *113*, 7227.
[19] H. E. Bunting, M. L. H. Green, S. R. Marder, M. E. Thompson, D. Bloor, P. V. Kolinsky, R. J. Jones, *Polyhedron* **1992**, *11*, 1489.
[20] J. Mata, E. Peris, I. Asselberghs, R. Van Boxel, A. Persoons, *New J. Chem.* **2001**, *25*, 299.
[21] H. Nock, H. Schottenberg, *J. Org. Chem.* **1993**, *58*, 7045.
[22] A. Houlton, N. Jasim, R. M. G. Rogerts, J. Silver, D. Cunningham, P. McArdle, T. Higgins, *J. Chem. Soc., Dalton Trans.* **1992**, 2235.
[23] V. Alain, A. Fort, M. Barzoukas, C.-T. Chen, M. Blanchard-Desce, S. R. Marder, J. W. Perry, *Inorg. Chim. Acta* **1996**, *242*, 43.
[24] D. R. Kanis, M. A. Ratner, T. J. Marks, *J. Am. Chem. Soc.* **1992**, *114*, 10338.
[25] I. R. Whittall, M. P. Cifuentes, M. J. Costigan, M. G. Humphrey, S. C. Goh, B. W. Skelton, A. H. White, *J. Organomet. Chem.* **1994**, *471,* 193.
[26] J. A. Bandy, H. E. Bunting, M.-H. García, M. L. H. Green, S. R. Marder, M. E. Thompson, D. Bloor, P. V. Kolinsky, R. J. Jones, J. W. Perry, *Polyhedron* **1992**, *11,* 1429.
[27] M. L. H. Green, S. R. Marder, M. E. Thompson, J. A. Bandy, D. Bloor, P. V. Kolinsky, R. J. Jones, *Nature* **1987**, *26*, 360.
[28] M. L. H. Greeen, J. Qin, D. O′Hare, H. E. Bunting, M. E. Thompson, S. R. Marder, K. Chatakondu, *Pure Appl. Chem.* **1989**, *61*, 817.
[29] M. Sheikh-Bahae, A. A. Said, T. Wei, D. J. Hagan, E. W. van Stryland, *IEEE J. Quant. Electr.* **1990**, 760.
[30] C. S. Winter, S. N. Oliver, J. D. Rush, *Nonlinear Optical Effects in Organic Polymers*, Kluwer, Dordrecht, **1989**.
[31] C. S. Winter, S. N. Oliver, J. D. Rush, *Optics Commun.* **1998**, *69*, 45.
[32] C. S. Winter, S. N. Oliver, J. D. Rush, *Organic Materials for Nonlinear Optics*, Royal Society of Chemistry, London, **1989**.
[33] S. Ghosal, M. Samoc, P. N. Prasad, J. J. Tufariello, *J. Phys. Chem.* **1990**, *94*, 2847.
[34] I. R. Whittall, M. G. Humphrey, M. Samoc, J. Swiatkiewicz, B. Luther-Davies, *Organometallics* **1995**, *14*, 5493.
[35] A. M. McDonagh, M. Cifuentes, I. R. Whittall, M. G. Humphrey, M. Samoc, B. Luther-Davies, D. C. R. Hockless, *J. Organomet. Chem.* **1996**, *526*, 99.
[36] I. R. Whittall, M. P. Cifuentes, M. G. Humphrey, B. Luther-Davies, M. Samoc, S. Houbrechts, A. Persoons, G. A. Heath, D. Bogsányi, *Organometallics* **1997**, *16,* 2631.
[37] I. R. Whittall, M. G. Humphrey, M. Samoc, B. Luther-Davies, *Angew. Chem. Int. Ed. Engl.* **1997**, *36*, 370.
[38] A. M. McDonagh, M. G. Humphrey, M. Samoc, B. Luther-Davies, S. Houbrechts, T. Wada, H. Sasabe, A. Persoons, *J. Am. Chem. Soc.* **1999**, *121*, 1405.
[39] A. M. McDonagh, M. G. Humphrey, M. Samoc, B. Luther-Davies, *Organometallics* **1999**, *18*, 5195.
[40] J. Vicente, M. T. Chicote, M. D. Abrisqueta, M. C. Ramírez de Arellano, P. G. Jones, M. G. Humphrey, M. P. Cifuentes, M. Samoc, B. Luther-Davies, *Organometallics* **2000**, *19*, 2968.
[41] W. H. Morrison, S. Krogsrud, D. N. Henrickson, *Inorg. Chem.* **1973**, *12*, 1998.
[42] K. R. J. Thomas, J. T. Lin, Y. S. Wen, *J. Organomet. Chem.* **1999**, *575*, 301.
[43] SAINT version 5.0, Bruker Analytical X-ray Systems, Madison, WI. G., **1998**.
[44] G. M. Sheldrick, University of Göttingen, **1996**.
[45] S. K. Kurtz, T. T. Perry, *J. Appl. Phys.* **1968**, *39*, 3798.

Received February 2, 2001
[I01069]